

Cite this: *Mater. Adv.*, 2023,  
4, 6439

## Stimuli-responsive chitosan-based injectable hydrogel for “on-demand” drug release†

Xiaoyu Wang,<sup>a</sup> Melissa Johnson,<sup>a</sup> Nan Zhang,<sup>b</sup> Pingping Shen,<sup>c</sup> Lizhu Yang,<sup>id d</sup>  
Cameron Milne,<sup>a</sup> Irene Lara-Sáez,<sup>id a</sup> Rijian Song,<sup>\*a</sup> Sigen A<sup>\*e</sup> and  
Wenxin Wang<sup>id a</sup>

Compared with traditional drug delivery systems, stimuli-responsive injectable hydrogels exhibit sol–gel transition in response to external stimuli, thus showing significant advantages in the on-demand release of drug molecules. Among them, chitosan-based stimuli-responsive injectable hydrogels have attracted considerable attention due to their excellent biocompatibility. However, the complex components, complicated preparation processes, and toxic chemical crosslinking agents make translating chitosan-based stimuli-responsive injectable hydrogels into clinical applications difficult. In this work, a facile and one-step method was developed to fabricate a stimuli-responsive chitosan-based injectable hydrogel based on the dynamic Schiff's base reaction. The hydrogel exhibited excellent stimuli-responsive properties and thixotropic features, including pH-responsive, self-healable, and injectable properties. Bovine serum albumin (BSA) and fluorescein isothiocyanate-dextran (FITC-dextran) were used as drug models to evaluate the on-demand release profiles of the hydrogel in different pH environments. The increased acidity triggers the release of both BSA and FITC-dextran from the hydrogel. No obvious cytotoxicity of the hydrogel extract was observed from Live/dead and alamarBlue assays on HEK 293 cells. The stimuli-responsive chitosan-based injectable hydrogel system is a promising candidate for on-demand drug release in response to pH stimuli.

Received 17th July 2023,  
Accepted 11th October 2023

DOI: 10.1039/d3ma00430a

rsc.li/materials-advances

## Introduction

Systemic administration typically causes low drug bioavailability and a rapid drop in plasma concentrations of drugs.<sup>1,2</sup> To overcome these drawbacks, on-demand drug release systems were developed in the past thirty years, aiming to deliver a therapeutic dose of drugs to the appropriate site of the body at a specific speed in a predetermined time, to promptly reach and maintain the desired drug concentration.<sup>3–5</sup> Compared with other systems, such as micelles and nano/microparticles, hydrogels normally possess excellent biocompatibility, biodegradability, and lower toxicity, thus gradually becoming a promising on-demand drug

release system and a viable alternative to overcome the shortcomings of traditional drug formulations.

Among various hydrogels, the emergence of injectable hydrogels has been a revolutionary breakthrough in the field of on-demand drug release due to their in-situ sol–gel conversion capabilities, biocompatibility, high water content, and biodegradability. In injectable hydrogel delivery systems, the drug and sol can be applied at the target position by injection. After the hydrogel is formed *in situ*, drugs are encapsulated in its network and then released through diffusion, which can maintain local high concentrations of drugs for a relatively long time to reduce the risk of side effects and patient discomfort.<sup>6–8</sup> Moreover, hydrogel networks can protect therapeutic components in hostile physiological environments, such as enzymes and low pH in some specific sites.<sup>4,9</sup> Injectable hydrogel delivery systems can also help to reduce surgical trauma and cost.<sup>10–16</sup> However, drug diffusion is generally passive or reliant on the natural degradation of hydrogels to release drugs. Currently, a common strategy to achieve on-demand release to give the drug delivery system the ability to receive signals spontaneously and rationally release the drug in response to environmental changes.

Stimuli-responsive hydrogels, also known as smart hydrogels, undergo significant changes in their swelling behaviour, network structure, permeability, or mechanical strength under

<sup>a</sup> Charles Institute of Dermatology, School of Medicine, University College Dublin, Dublin D04 V1W8, Ireland. E-mail: [sigen.a@aust.edu.cn](mailto:sigen.a@aust.edu.cn)

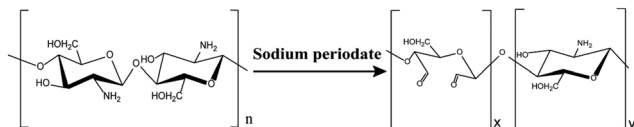
<sup>b</sup> Centre of Micro/Nano Manufacturing Technology (MNMT-Dublin), School of Mechanical and Materials Engineering, University College Dublin, Dublin D04 KW52, Ireland

<sup>c</sup> State Key Laboratory of Pharmaceutical Biotechnology, School of Life Sciences, Nanjing University, Nanjing, Jiangsu, 210023, P.R. China

<sup>d</sup> School of Pharmaceutical Sciences, Wenzhou Medical University, Wenzhou, Zhejiang, 325035, P.R. China

<sup>e</sup> School of Medicine, Anhui University of Science and Technology, Huainan, Anhui, 232001, P.R. China

† Electronic supplementary information (ESI) available. See DOI: <https://doi.org/10.1039/d3ma00430a>



**Scheme 1** The oxidation reaction between chitosan (CTS) and sodium periodate and the structure of aldehyde chitosan (CTS-CHO).

external stimulations, such as temperature, pH, light, and electromagnetic fields. Therefore, the drugs embedded in stimuli-responsive hydrogels can be released in an on-demand manner.<sup>17</sup> pH-responsive hydrogels are a type of stimuli-responsive hydrogel that is currently of widespread interest because they can rapidly release the drug in a targeted acidic site while minimising drug release in normal physiological environments.<sup>18–20</sup>

Chitosan (CTS) is a natural cationic polymer which derives from chitin through deacetylation. The chemical structure of CTS is composed of glucosamine (2-amino-2-deoxy-d-glucose) and N-acetyl glucosamine (as shown in Scheme 1).<sup>21</sup> CTS-based hydrogels have attracted increasing attention for on-demand drug release due to its renewable resources, non-toxicity, high biodegradability, and good biocompatibility.<sup>22</sup> However, the poor solubility and mechanical strength still need to be overcome. Aldehyde chitosan (CTS-CHO) which is synthesised from CTS through the oxidation reaction has been reported in some literature.<sup>23–26</sup> The greatly improved solubility, well-maintained biological activity, and self-crosslinking properties allow CTS-CHO to be a great alternative to CTS for on-demand drug release applications. Although CTS-based hydrogels have been widely reported, the stimuli-responsive injectable hydrogel which is fabricated from CTS-CHO used for on-demand drug release is rarely reported.

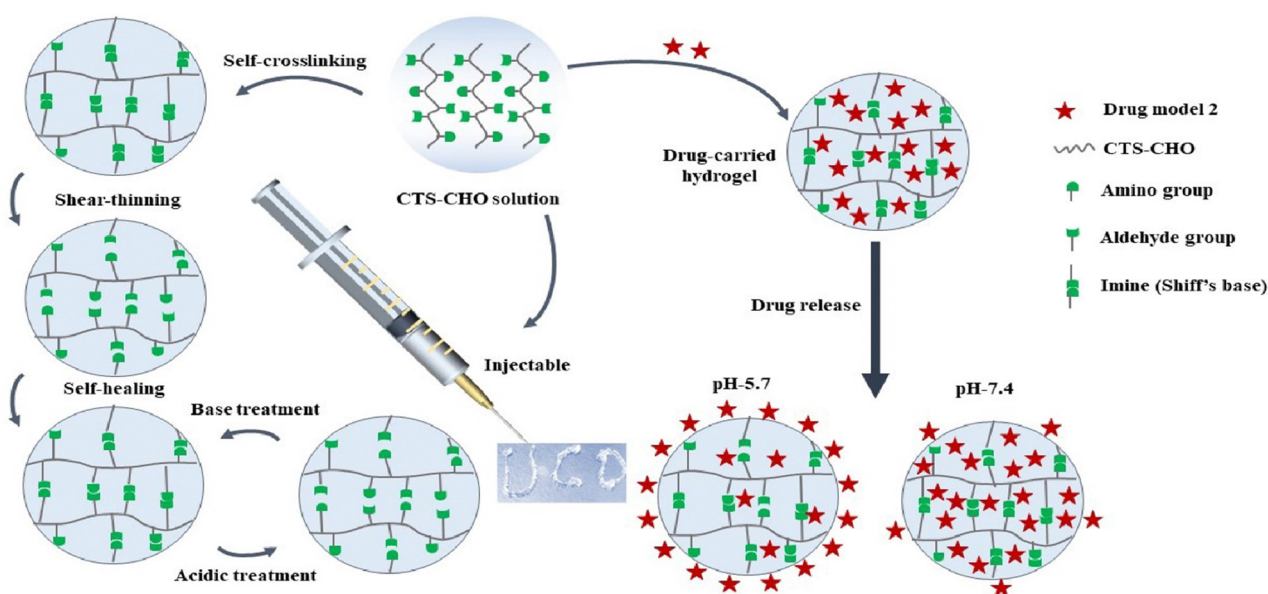
Here, we designed a stimuli-responsive injectable hydrogel with CTS-CHO for on-demand drug release. CTS-CHO was

prepared by oxidation of CTS using sodium periodate (Scheme 1). The hydrogels were fabricated with CTS-CHO by adjusting the concentration under the neutral condition. The process of stimuli-responsive hydrogel study in this work is outlined in Scheme 2, which includes the preparation and characterisation of the hydrogel. The stimuli-responsive performance, rheological behaviours, swelling, and degradation profiles, and *in vitro* on-demand drug release profiles were assessed. The release rates of BSA and FITC-dextran from the hydrogel were significantly accelerated when the pH of phosphate-buffered saline was reduced from 7.4 to 5.7 due to the pH-responsive property. In addition, the cytotoxicity of the hydrogel was estimated against HEK 293 cells using alamarBlue assay and Live/dead assay. No obvious cytotoxicity of the hydrogel extract was observed. The stimuli-responsive chitosan-based injectable hydrogel system is a promising candidate for on-demand drug release in response to pH stimuli.

## Experimental procedure

### Materials

CTS (medium molecular weight, 75–85% deacetylation degree), fluorescein isothiocyanate-dextran ( $M_w$ : 2000 kDa) and bovine serum albumin (BSA) were purchased from Sigma-Aldrich. Dialysis tubes (cut off  $M_w$ : 8 kDa) were purchased from Spectrum-Lab. Glacial acetic acid, sodium periodate, BCA protein assay kit, phenol red, deuterated acetic acid ( $C_2H_4O_2$ , 99.5%) and ethylene glycol were purchased from Thermo Scientific. The HEK 293 cell line was purchased from ATCC. Live/Dead Viability Cytotoxicity Kit was purchased from BioScience. AlamarBlue reagent and deuterium oxide ( $D_2O$ , 99.9%) were provided by Sigma-Aldrich. Penicillin/streptomycin, fetal bovine serum (FBS), and Dulbecco's Modified Eagle's Medium (DMEM) were purchased from Invitrogen. All materials were used as received.



**Scheme 2** Multi-responsive properties of the Schiff's base and drug release profiles of CTS-CHO hydrogel.



### Synthesis of dialdehyde chitosan

CTS-CHO was synthesised according to our previous study.<sup>27</sup> Briefly, 0.97 g of CTS was dissolved in 100 mL of 0.1 mol L<sup>-1</sup> acetic acid solution and stirred continuously for 24 hours at room temperature. Then 0.64 g of sodium periodate was added to the CTS solution and stirred for 24 hours in the dark. Ethylene glycol (0.5 mL) was then added to the solution and 1 hour of stirring was conducted to terminate the reaction. The solution was dialysed 5 times against 5L deionised water, and the deionised water was changed every 4 hours. The purified solution was filtered with filter paper. The dialysate was lyophilised for 3 days to obtain CTS-CHO.

### Proton nuclear magnetic resonance (<sup>1</sup>H NMR)

10 mg of both CTS and CTS-CHO were individually dissolved in 750 µL of D<sub>2</sub>O. Subsequently, 40 µL of C<sub>2</sub>H<sub>4</sub>O<sub>2</sub> was introduced into each vial, followed by vortexing for 10 minutes. The acquisition of <sup>1</sup>H-NMR spectra was conducted using a Varian 400 MHz NMR spectrometer.

### Element analysis

The quantitative flash combustion technique was used for the element analysis. The analysis was conducted on an Exeter elemental analyser (CE440, Coventry, United Kingdom) with a typical sample of 1.6–1.9 mg weighed on a Sartorius ultra-micro balance. The polymer samples were thoroughly dried by lyophilisation for 3 days before analysis. The oxidation degree ( $F_{ox}$ ) was calculated following the equation:

$$\frac{N}{C} = \frac{F_A + (1 - F_A) \cdot (1 - F_{ox})}{2F_A + 6} \quad (1)$$

where  $F_A$  is the acetylated units' content in chitosan.  $N$  and  $C$  is the percentage of nitrogen and carbon, respectively.

### Preparation of CTS-CHO self-crosslinked hydrogel

CTS-CHO was dissolved in deionised water to the desired concentrations (10%, 11%, and 12%), and then the hydrogels formed after a certain time.

### Gelation time

1 mL of CTS-CHO solution was placed in glass vials to observe the gelation profiles. The inverted tube method was used to record the gelation time of the hydrogels.

### pH-responsive property

1 mL of CTS-CHO solution at a concentration of 10% was placed in a glass vial. After the hydrogel formation, 10 µL of 2 M HCl was added to the vial and observed. When the hydrogel became a solution, 10 µL of 2 M NaOH was added to the same vial, and then observed again. Photos were taken when the sol-gel transition occurred.

### Injectability

CTS-CHO was dissolved to a concentration of 10% in deionised water and 0.02% aqueous solution of phenol red. The CTS-CHO

solution in the syringe (22 G needle) was kept at room temperature for 24 hours. The hydrogel was then extruded, and photos were taken.

### Rheological parameters

Discovery HR-2 Rheometer (TA Instrument, HR-2, New Castle, Delaware, USA) was used to analyse the viscoelastic behaviours of CTS-CHO hydrogels at 25 °C. The diameter of the parallel plate geometry used in this experiment was 8 mm. After 24 hours, 200 µL of CTS-CHO hydrogel was analysed for each test. The gap was set as 2 mm. Firstly, the storage modulus ( $G'$ ) of the hydrogels at the concentration of 10%, 11%, and 12% was evaluated. The linear viscoelastic range of the hydrogels was evaluated using a strain sweep test at a frequency of 1 Hz. Then, the hydrogels were subjected to 500% strain and 1% strain for 4 cycles, and the variations in storage modulus and complex viscosity were recorded. In addition, shear rate scans were performed to investigate the shear thinning behaviour of hydrogels subjected to shear rates ranging from 0.01–100 l s<sup>-1</sup>. Each experiment was performed in triplicate.

### Swelling

At 37 °C, 0.2 g of hydrogels were immersed in 20 mL PBS at a pH of 7.4). At the predetermined time points, the water on the surface of the samples was carefully removed with filter paper. The hydrogels were weighed. After weighing at each time point, PBS was replaced with a newly prepared solution.

The swelling ratio (SR) was calculated following the formula:

$$SR = \frac{W_t}{W_0} \quad (2)$$

$W_0$  is the initial hydrogel weight.  $W_t$  is the hydrogel weight at the predetermined time  $t$ .

### In vitro degradation

20 mL PBS (pH 5.7, 7.4) was used to immerse 0.2 g of hydrogels at 37 °C. Then at pre-determined time points, the water on the surface of the residual samples was removed carefully with filter paper. The weight of the hydrogel was recorded. After weighing at each time point, PBS was replaced with a newly prepared solution:

$$DR\% = \frac{(W_0 - W_t)}{W_0} \times 100 \quad (3)$$

$W_0$  is the initial hydrogel weight.  $W_t$  is the residual hydrogel weight at the degradation time  $t$ .

### In vitro BSA release

50 mL of deionised water was used to dissolve 2 g of BSA to obtain a 4% BSA solution. BSA solution was diluted to 0.1, 0.2, 0.4, 0.6, 0.8, 1.0, and 2.0 mg mL<sup>-1</sup> concentrations. The negative control was PBS (pH 7.4). The working reagent was prepared following the user guide of the BCA protein assay kit. Then 25 µL of each standard and negative control sample were placed in a microplate (96-well). 200 µL of the working reagent was then added. Next, the 96-well microplate was mixed for



30 seconds and then incubated for 30 minutes at 37 °C. The absorbance at 562 nm was measured using a microplate reader (SpectraMax M3, Molecular Devices, Inc., USA) after the microplate was cooled to room temperature. The average absorbance of each BSA standard and its concentration were used to prepare the standard curve.

CTS-CHO was dissolved in 4% BSA solution to the concentrations of 10% and 11%. The CTS-CHO solution was then left at room temperature for 24 hours to ensure complete gelation. In 5 mL PBS (pH 5.7 and 7.4), 0.1 g hydrogel was immersed. As a negative control, a hydrogel prepared with deionised water was used. The BSA-loaded hydrogel and negative control sample were incubated at 37 °C. An equal amount of fresh PBS was replenished after the collection of 1 mL aliquots at predetermined time intervals. The standard curve was used to calculate the protein concentration. The cumulative release was then calculated according to the equation below:

$$\text{Cumulative release\%} = \frac{(C_t - C_0) \times 5 + C_{(t-1)}}{m \times 40} \times 100\% \quad (4)$$

$C_0$  is the protein concentration of negative control.  $C_t$  is the protein concentration of BSA-loaded hydrogel at a predetermined time  $t$ .  $C_{(t-1)}$  is the protein concentration of BSA-loaded hydrogel at the time point before time  $t$ .  $m$  is the initial weight of the hydrogel.

#### *In vitro* FITC-dextran release

40 mg FITC-dextran was dissolved in 10 mL deionised water to obtain a 4 mg mL<sup>-1</sup> FITC-dextran solution. Diluted FITC-dextran solutions were prepared at concentrations of 3.125, 6.25, 12.5, 25, 50, 100, and 200 µg mL<sup>-1</sup>. The negative control was PBS (pH 7.4). Then, 100 µL of the standard and negative control sample was placed in a 96-well microplate. According to the user guide, the emission maximum is 520 nm, and the excitation maximum is 490 nm. The fluorescence was measured by a Microplate reader. The average absorbance of each dextran standard and its concentration were used to prepare the standard curve.

CTS-CHO was dissolved in 4 mg mL<sup>-1</sup> FITC-dextran solution to the concentrations of 10% and 11%. Then the CTS-CHO solution was left for 24 hours at room temperature to ensure complete gelation. 0.1 g hydrogel was immersed in 5 mL PBS (pH 5.7 and 7.4). The hydrogel prepared with deionised water was used as the negative control. The dextran-loaded hydrogel and negative control sample were incubated at 37 °C. An equal amount of fresh PBS was replenished after the collection of 1 mL aliquots at predetermined time intervals. The standard curve was used to calculate the dextran concentration.

The cumulative release was calculated according to the equation below:

$$\text{Cumulative release\%} = \frac{(C_t - C_0) \times 5 + C_{(t-1)}}{m \times 4 \times 1000} \times 100\% \quad (5)$$

$C_0$  is the dextran concentration of negative control.  $C_t$  is the dextran concentration of dextran-loaded hydrogel at a predetermined time  $t$ .  $C_{(t-1)}$  is the dextran concentration of dextran-loaded

hydrogel at the time point before time  $t$ .  $m$  is the initial weight of the hydrogel.

#### *In vitro* cytotoxicity assessment

The cytotoxicity of CTS-CHO self-crosslinked hydrogels was determined using HEK 293 cells by alamarBlue assay and Live/Dead staining assay.

Briefly, 1000 mg CTS-CHO hydrogel was immersed in 10 mL DMEM (containing 10% FBS, 1% penicillin) and incubated at 5% CO<sub>2</sub>, 37 °C for 24 hours. The supernatant was filtered for sterilisation using a 0.22 µm filter, and then the stock extract solution (100%) was obtained. The stock extract solution was diluted to 50%, 25%, and 12.5% with DMEM. HEK 293 cells at the density of  $1 \times 10^4$  cells well<sup>-1</sup> were seeded in a 96-well microplate, and then cultured at 5% CO<sub>2</sub> and 37 °C for 24 hours. The medium was replaced with 100 µL extract solution. After incubation for 24 hours, 20 µL alamarBlue reagent was added and then incubated at 37 °C for 4 hours. The fluorescence was read using a fluorescence excitation wavelength of 570 nm by a Microplate reader. Cells with DMEM containing alamarBlue reagent were the negative control group. The cell viability was calculated following the equation:

$$\text{Cell viability} = \frac{F_s}{F_c} \times 100\% \quad (6)$$

$F_s$  is the fluorescence value of the sample.  $F_c$  is the fluorescence value of the control.

As for the Live/Dead staining assay, the stock extraction solution was prepared with the same method as the alamarBlue assay. The stock solution was diluted to 50% and 25% with DMEM. HEK 293 cells ( $1 \times 10^4$  cells well<sup>-1</sup>) were seeded in a 96-well microplate and then cultured at 5% CO<sub>2</sub> and 37 °C for 24 hours. Next, the culture medium was replaced with a 100 µL extraction solution. After incubation for 24 hours, the live/dead stain reagent was pre-thawed. According to the user guide, 2 µL calcein-AM and 8 µL ethidium homodimer-1 were mixed with 4 mL DPBS, then the Live/Dead staining solution was obtained. Then the culture medium was replaced with 100 µL of the staining solution. After incubation for 30 minutes at 20 to 25 °C, DPBS was used to wash the cells. Then photographs were taken under a fluorescence microscope.

#### Statistical analysis

All data are presented as mean ± standard deviation. The difference between individual groups was assessed using one-way or two-way analysis of variance and Tukey's post-analysis. The statistical significance was considered with a p-value of less than 0.05. The analysis of the data was performed using GraphPad Prism 7 software (GraphPad Software, USA).

## Results and discussion

In this work, we designed a stimuli-responsive hydrogel composed of CTS-CHO for on-demand drug release. Aldehyde groups were introduced in the structure of chitosan *via* oxidation reaction following the previous procedure we reported.<sup>27</sup>





CTS-CHO hydrogels with stimuli-responsive properties were obtained by adjusting the concentration in a neutral condition.

To confirm that the functionalisation was successful,  $^1\text{H}$  NMR was used to characterise the structures of CTS and CTS-CHO. The spectra were shown in Fig. S1 (ESI $^\dagger$ ). The new peaks of  $^1\text{H}$  NMR spectra at 8 ppm correspond to hemiacetalic protons derived from the aldehyde groups and neighbouring hydroxyl groups. This characteristic aldehyde-based peak was only evident in the CTS spectrum post-oxidation. This result demonstrated that aldehyde groups were introduced into the structure of CTS after the oxidation reaction successfully. The result is consistent with the literature.<sup>28,29</sup> The C2-C3 linkage was cleaved in the *N*-acetyl-glucosamine unit (GlcN) and dialdehyde was formed.

An element analyser was used to test the percentages of C, N, and H in the structure of CTS-CHO. According to the literature, the oxidation degree was calculated according to eqn (1) and the result was 11.32%, as shown in Table S1 (ESI $^\dagger$ ). The percentage of dialdehyde per 100 GlcN units is the oxidation degree of CTS-CHO.<sup>25</sup> Another promising property of CTS-CHO is that its water solubility improved significantly when compared to CTS. Presumably, the hydration of aldehyde groups in the structure considerably increased the solubility of CTS-CHO dramatically.

Gelation times of CTS-CHO hydrogels at the concentration of 10%, 11%, and 12% were determined using the inverted tube method at room temperature. Fig. S2 (ESI $^\dagger$ ) shows that the average gelation time at 10% concentration was 20 minutes, 3 minutes at 11%, and 30 seconds at 12% concentration. The storage modulus of CTS-CHO hydrogels at concentrations of 10%, 11%, and 12% was tested to evaluate the mechanical strength. The results were shown in Fig. S3 (ESI $^\dagger$ ), 294, 817, and 953 Pa, respectively.

The mechanical strength of the hydrogel increased with the concentration of CTS-CHO. As shown in Fig. 1(a), the strain sweep results showed the strain that broke the hydrogel network was 300%.  $G'$  was higher than  $G''$  in the strain range of 1% to 300%, indicating the solid structure of the hydrogel. Whereas  $G'$  decreased below  $G''$  when the strain was above 300%, which means that the structure of the hydrogel was disrupted. The shear rate sweep measurement was performed, and the results confirmed the shear thinning behaviour of the gel for injectability (Fig. 1b).

The results of cyclic strain sweep tests (Fig. 2) showed that  $G'$  and complex viscosity recovered when the high strain (500%) is removed for 60 seconds, and this process could be repeated several times. This recovery behaviour indicated the dynamic

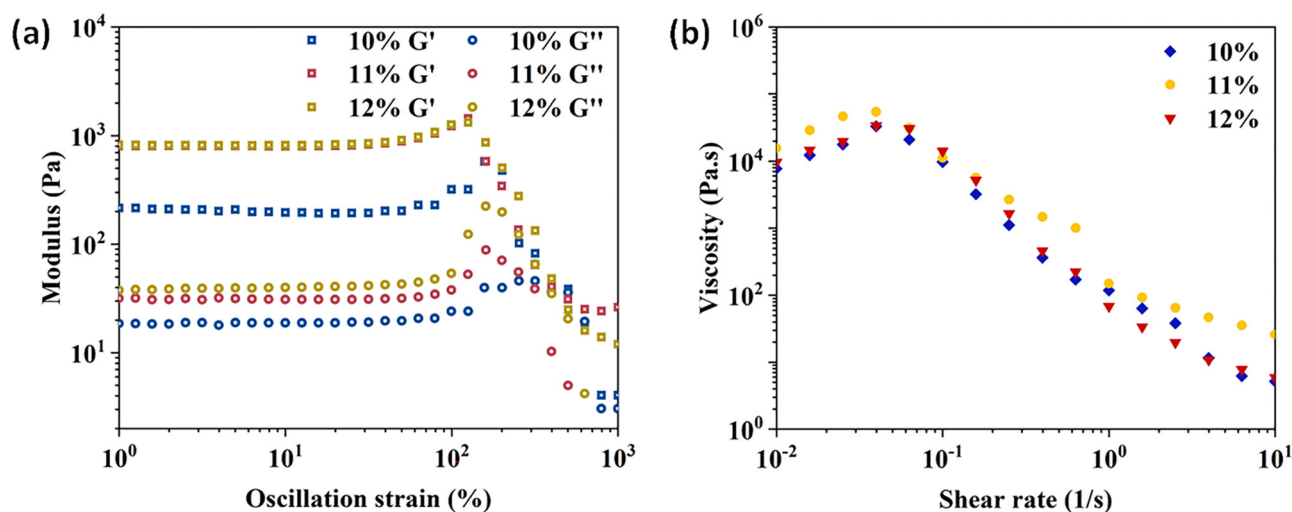


Fig. 1 Rheological properties of CTS-CHO hydrogels. (a) Strain sweep of the hydrogels at the concentration of 10%, 11%, and 12%. (b) Viscosity change of the hydrogels as a function of shear.

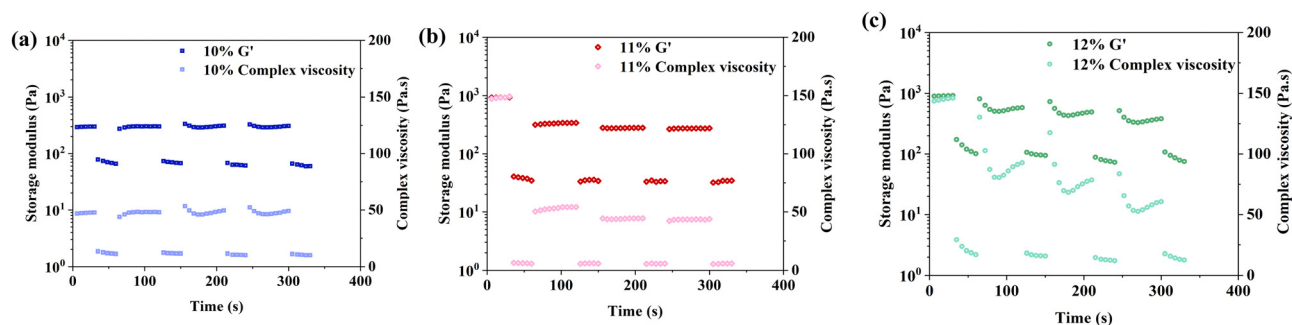


Fig. 2 Dynamic step-strain amplitude measurements of the hydrogels. (a) 10%; (b) 11%; (c) 12%.

covalent bonds (imine linkages) reformed after a high-strain disruption.<sup>30,31</sup> However, during dynamic testing, the hydrogel may not have enough time to fully heal between strain cycles. As a result, the accumulated damage from each cycle leads to a gradual decrease in storage modulus over time.

After adding 10  $\mu$ L HCl (2 M) to the vial, the hydrogel turned into a solution in 30 minutes. the hydrogel formed in 30 minutes again when 10  $\mu$ L NaOH (2 M) was added to the vial (Fig. 3a and b). This sol-gel transition phenomenon confirmed that the CTS-CHO hydrogel was pH-responsive. CTS-CHO was dissolved in deionised water and a dyed aqueous solution to a concentration of 10%. After 24 hours, the hydrogel was extruded through a syringe with a 22 G needle (Fig. 3c and d), indicating that the hydrogel had excellent injectable properties.

The self-healable, injectable, and pH-responsive properties of CTS-CHO hydrogel are advantageous for controlled drug release, allowing it to be used as a drug carrier.

The degradation profiles of the CTS-CHO hydrogels were assessed in PBS at pH 5.7 and 7.4. In pH 7.4 PBS, 38% and 40% of the initial weights of the 11% and 12% hydrogels were retained, respectively. Whereas the 10% hydrogel degraded completely in 3 days, due to the low crosslinking density (Fig. 4a). In pH 5.7 PBS, the hydrogels degraded gradually after slight swelling and then degraded completely in 5 hours (Fig. 4b), because the imine linkages formed between aldehyde and amino groups are dynamic, reversible, and easily hydrolysed under acidic conditions. At each time point, the remaining weight of the high-concentration hydrogel was slightly greater than the low-concentration hydrogel. The swelling behaviour of CTS-CHO hydrogel was conducted at 37  $^{\circ}$ C in

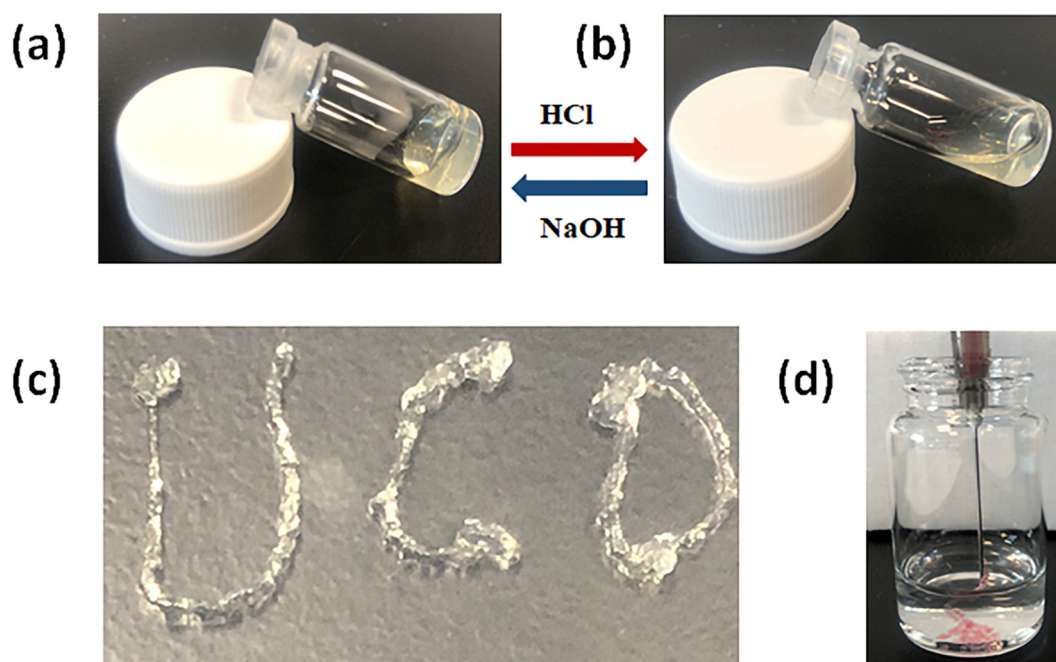


Fig. 3 Multi-responsive properties of CTS-CHO self-crosslinked hydrogels. (a) and (b) pH-responsive property. (c) and (d) Injectability.

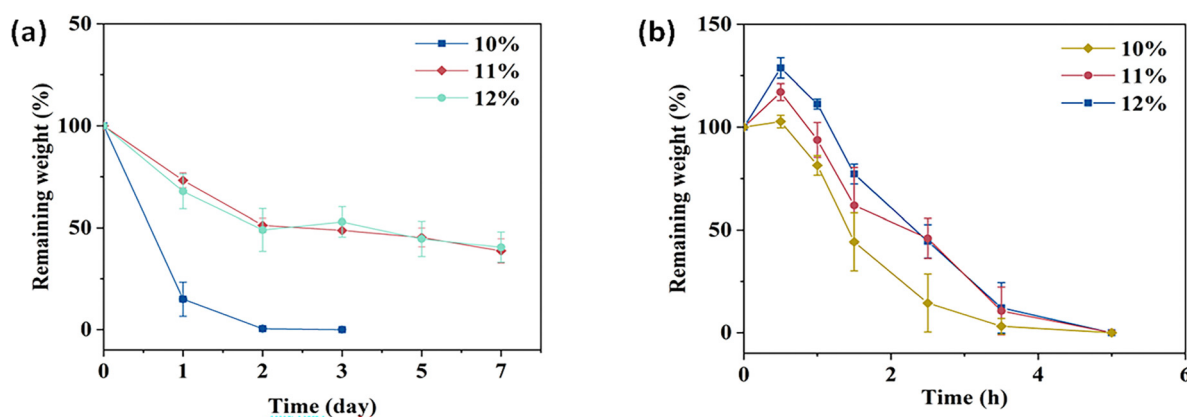


Fig. 4 (a) Degradation profiles of CTS-CHO self-crosslinked hydrogels in pH 7.4 PBS. (b) Degradation profiles of CTS-CHO self-crosslinked hydrogels in pH 5.7 PBS. Data in the figure are the average value of  $n = 3$ ,  $\pm$  standard deviation.



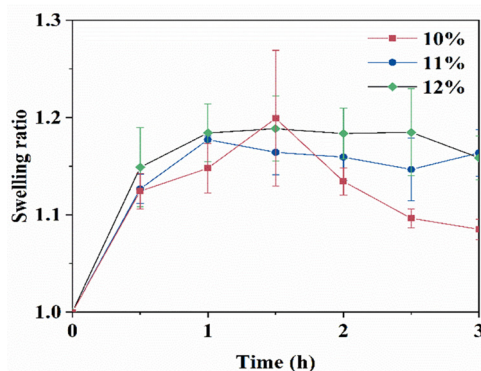


Fig. 5 Swelling of CTS-CHO self-crosslinked hydrogels in pH 7.4 PBS. Data in the figure are the average value of  $n = 3$ ,  $\pm$  standard deviation.

pH 7.4, PBS. In Fig. 5, the equilibrium swelling ratio of the 11% and 12% hydrogels was around 1.2, and no significant difference was observed in these two groups. As for the 10% hydrogel, the swelling ratio reached about 1.2 in 1.5 hours, and then degradation was observed. Crosslinking density is a crucial factor that affects the swelling profile of the hydrogel. The equilibrium swelling of the 10% hydrogel was maintained for a shorter time than the 11% and 12% hydrogels due to the low concentration of CTS-CHO. Due to the

similar swelling and degradation profiles of the 11% and 12% hydrogels, the 10% and 11% hydrogels were selected for further *in vitro* drug release studies.

BSA and FITC-dextran as model drugs were encapsulated in the hydrogels and on-demand drug release behaviours at different pH were observed, as shown in Fig. 6. In PBS at pH 7.4, BSA and FITC-dextran were released from the 10% and 11% hydrogels gradually in the first 6 hours (Fig. S4 and S5, ESI†). The cumulative release of BSA reached around 67% and 46% in 24 hours, followed by a sustained and slow release for 2 days. The 11% hydrogel released BSA slower than the 10% hydrogel due to the higher crosslinking density. At 48 hours, the cumulative BSA release of the 10% hydrogel was 72%, and that of the 11% hydrogel was still around 50% (Fig. 6a). Compared with the cumulative BSA release ratio of other hydrogels in the literature, that of the 10% CTS-CHO hydrogel at 48 hours was lower.<sup>32,33</sup> The BSA release rate in pH 5.7 PBS was shown in Fig. 6(b). BSA was released from CTS-CHO hydrogel relatively fast in the first hour, and then a slow release was observed later. In 2 hours, 82% and 69% of BSA were released from the hydrogels at the concentration of 10% and 11%, respectively. That may be due to the hydrolysis of reversible dynamic imine linkages between the amino groups in BSA.

At 24 hours, the FITC-dextran release levels were 73% and 67% for the 10% and 11% hydrogels in pH 7.4 PBS, as shown in

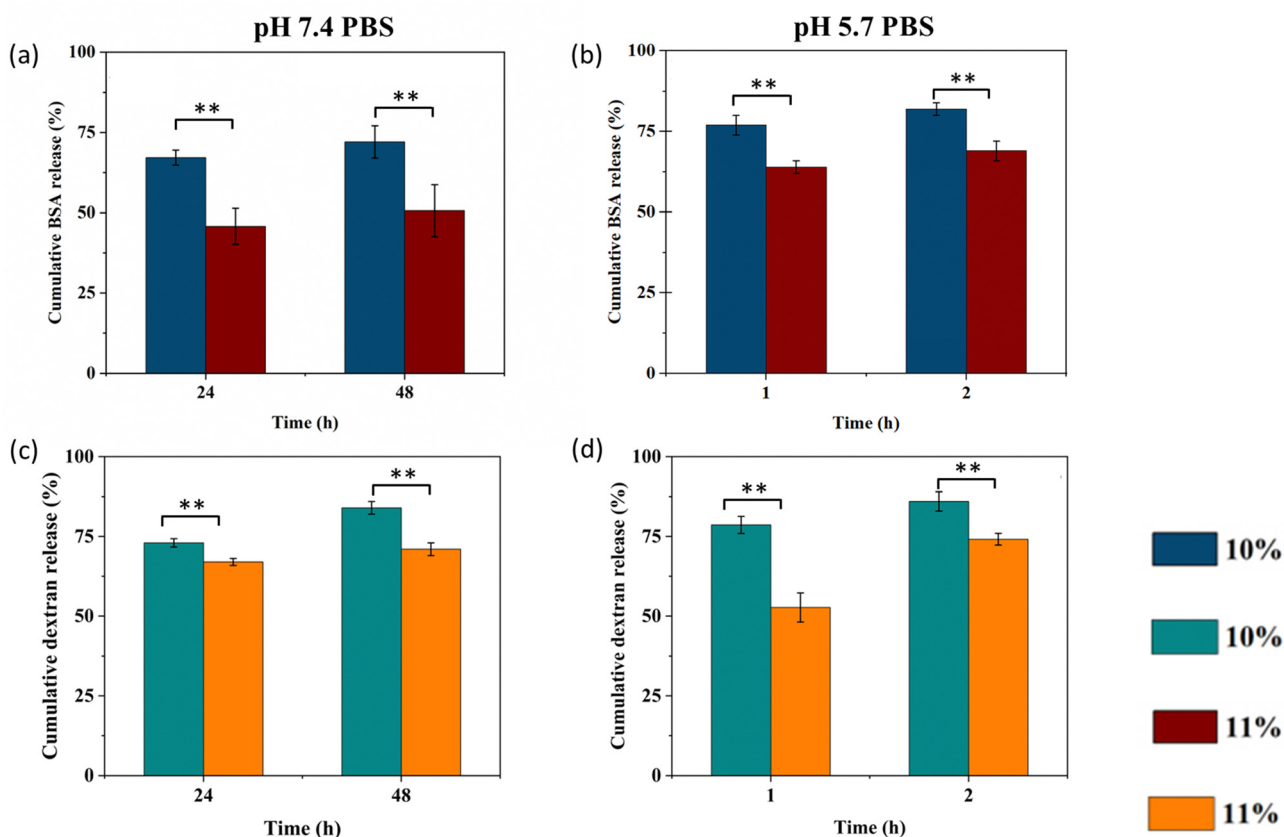
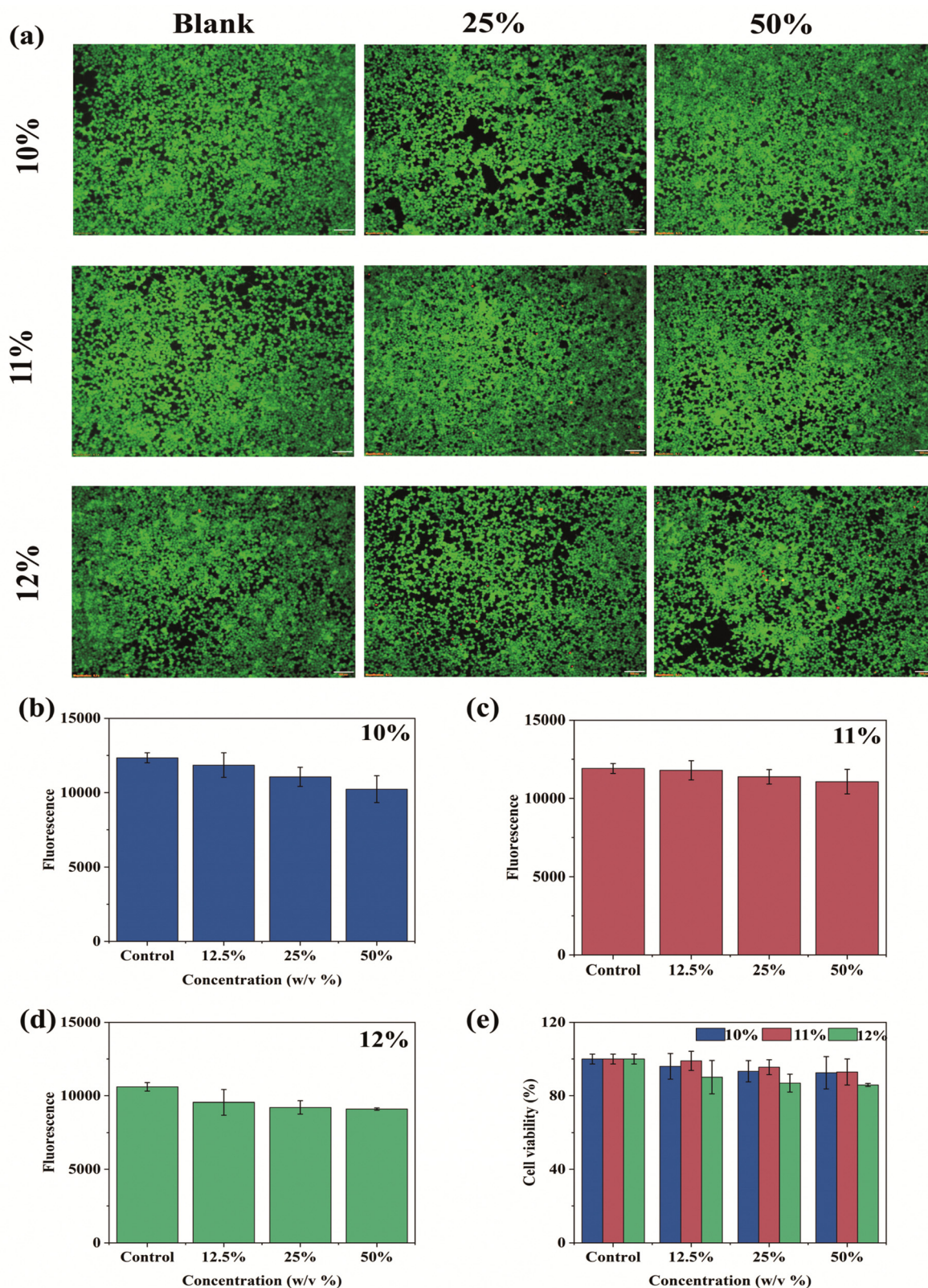


Fig. 6 Drug release profile in PBS (pH 5.7, and 7.4). (a) BSA release in pH 7.4 PBS after 24 and 48 hours. (b) BSA release in pH 5.7 PBS after 1 and 2 hours. (c) FITC-dextran release in pH 7.4 PBS after 24 and 48 hours. (d) FITC-dextran release in pH 5.7 PBS after 1 and 2 hours. Data in the figure are the average value of  $n = 3$ ,  $\pm$  standard deviation. \* $p < 0.05$ , \*\* $p < 0.01$ .







**Fig. 7** Cytotoxicity of CTS-CHO self-crosslinked hydrogel. (a) Live/Dead staining of HEK 293 cells treated with the extract of the hydrogel. (b)–(e) AlamarBlue measurements of HEK 293 cells co-cultured with the hydrogel extract. Data in the figure are the average value of  $n = 3$ ,  $\pm$  standard deviation. Scale bar: 100  $\mu$ m.





Fig. 6(c). At 48 hours, the cumulative release of FITC-dextran was around 84% from the 10% and 71% from the 11% hydrogels respectively. Fig. 6(d) shows that after 2 hours of incubation, the FITC-dextran release level was 86% and 74% for the 10% and 11% hydrogels loaded with FITC-dextran in pH 5.7 PBS, respectively. FITC-dextran released from CTS-CHO hydrogel through diffusion. The on-demand release capability demonstrated that the CTS-CHO hydrogel is a promising candidate in the drug delivery field.

CTS-CHO is non-cytotoxic according to our previous report.<sup>27</sup> To evaluate the cytotoxicity of CTS-CHO hydrogel, alamarBlue assay and Live/Dead staining assay were conducted on HEK 293 cells by treating cells with hydrogel extract for 24 hours (Fig. 7). In Fig. 7(a), the fluorescence microscopy images of Live/Dead staining demonstrated that the majority of HEK 293 cells were viable with intact morphology after 24 hours of treatment with hydrogel extract. No significant difference from the controls was observed. Overall, the results indicated that the extract of CTS-CHO self-crosslinked hydrogel did not affect the viability of HEK 293 cells. According to the results of alamarBlue assay, the cell viability of CTS-CHO self-crosslinked hydrogel at various experimental concentrations was above 80% (Fig. 7b–e). Biomaterials for medical applications should be biocompatible and are normally considered non-cytotoxic if the cell viability is higher than 70% after 24 hours of co-incubation with cells.<sup>34,35</sup> Hence, based on this recommendation, CTS-CHO hydrogel was non-cytotoxic.

## Conclusions

In this study, an injectable hydrogel system with stimuli-responsive properties was reported. The hydrogel was prepared with CTS-CHO, which was synthesised *via* oxidation reaction with CTS and sodium periodate, by adjusting the concentration. Moreover, the hydrogel system also possesses crucial properties for on-demand release, such as degradability, injectability, self-healing, and biocompatibility.

The model drugs, BSA and FITC-dextran were released from CTS-CHO hydrogel relatively fast in pH 5.7 PBS and more slowly in pH 7.4 PBS. No obvious cytotoxicity of the hydrogel extract was observed from Live/dead and alamarBlue assays on HEK 293 cells. The stimuli-responsive chitosan-based injectable hydrogel system is a promising candidate for on-demand drug release in response to pH stimuli. Moreover, the pH-responsive property of CTS-CHO hydrogels were reported for the first time, which indicated the huge potential of CTS-CHO in the biomedical field.

## Author contributions

Conceptualisation, XW; methodology and validation, XW, NZ, RS and PS; investigation and data curation, XW; writing – original draft preparation, XW; writing – review & editing, MJ, ILS and CM; sources, WW; project administration, supervision and funding acquisition SA. All authors have read and agreed with the final manuscript.

## Conflicts of interest

There are no conflicts to declare.

## Acknowledgements

This research was funded by China Scholarship Council (CSC202009110089), and Science Foundation Ireland (SFI) (Funding Agency Ref No: 19/FFP/6522).

## References

- 1 A. Kidane and P. P. Bhatt, *Curr. Opin. Chem. Biol.*, 2005, **9**, 347–351.
- 2 N. Bhattarai, J. Gunn and M. Zhang, *Adv. Drug Delivery Rev.*, 2019, **62**, 83–99.
- 3 Y. Qiu and K. Park, *Adv. Drug Delivery Rev.*, 2012, **64**, 321–339.
- 4 M. Vigata, C. Meinert, D. W. Hutmacher and N. Bock, *Pharmaceutics*, 2020, **12**, 1188.
- 5 G. Ahuja and K. Pathak, *Indian J. Pharm. Sci.*, 2009, **71**, 599–607.
- 6 M. Gulfam, S.-H. Jo, S.-W. Jo, T. T. Vu, S.-H. Park and K. T. Lim, *NPG Asia Mater.*, 2022, **14**, 8.
- 7 J. Hu, C. Zhang, L. Zhou, Q. Hu, Y. Kong, D. Song, Y. Cheng and Y. Zhang, *Sci. China Mater.*, 2020, **64**, 1035–1046.
- 8 J. Zhao, X. Liang, H. Cao and T. Tan, *Bioresources Bioprocess.*, 2020, **7**, 1.
- 9 S. Noppakundilgrat, S. Choopromkaw and S. Kiatkamjornwong, *J. Appl. Polym. Sci.*, 2018, **135**, 45654.
- 10 M. K. Nguyen and D. S. Lee, *Macromol. Biosci.*, 2010, **10**, 563–579.
- 11 J. Qu, X. Zhao, P. X. Ma and B. Guo, *Acta Biomater.*, 2017, **58**, 168–180.
- 12 Y. Gao, A. Deng, X. Wu, C. Sun and C. Qi, *React. Funct. Polym.*, 2021, **161**, 104866.
- 13 M. S. Gil, T. Thambi, V. H. G. Phan, S. H. Kim and D. S. Lee, *J. Mater. Chem. B*, 2017, **5**, 7140–7152.
- 14 H. Jang, K. Zhi, J. Wang, H. Zhao, B. Li and X. Yang, *Int. J. Biol. Macromol.*, 2020, **148**, 163–172.
- 15 Y. S. Jung, W. Park, H. Park, D. K. Lee and K. Na, *Carbohydr. Polym.*, 2017, **156**, 403–408.
- 16 R. Li, Y. Zhang, Z. Lin, Q. Lei, Y. Liu, X. Li, M. Liu, G. Wu, S. Luo, H. Wang, X. Zhang, L. Li, N. Ao and Z. Zha, *Composites, Part B*, 2021, **221**, 109031.
- 17 M. Fathi, P. S. Zangabad, S. Majidi, J. Barar, H. Erfan-Niya and Y. Omid, *Bioimpacts*, 2017, **7**, 269–277.
- 18 F. F. Azhar, E. Shahbazzpour and A. Olad, *Fibers Polym.*, 2017, **18**, 416–423.
- 19 X. Bao, X. Si, X. Ding, L. Duan and C. Xiao, *J. Polym. Res.*, 2019, **26**, 278.
- 20 H. Hamed, S. Moradi, S. M. Hudson and A. E. Tonelli, *Carbohydr. Polym.*, 2018, **199**, 445–460.
- 21 M. George and T. E. Abraham, *J. Controlled Release*, 2006, **114**, 1–14.



- 22 O. Guaresti, C. Garcia-Astrain, R. H. Aguirresarobe, A. Eceiza and N. Gabilondo, *Carbohydr. Polym.*, 2018, **183**, 278–286.
- 23 X. Liu, N. Dan, W. Dan and J. Gong, *Int. J. Biol. Macromol.*, 2016, **82**, 989–997.
- 24 P. Bam, A. Bhatta and G. Krishnamoorthy, *Int. J. Biol. Macromol.*, 2019, **130**, 836–844.
- 25 I. Charhouf, A. Bennamara, A. Abourriche, A. Chenite, J. Zhu and M. Berrada, *Int. J. Sci.: Basic Appl. Res.*, 2014, **16**, 336–348.
- 26 I. M. N. Vold and B. E. Christensen, *Carbohydr. Res.*, 2005, **340**, 679–684.
- 27 X. Wang, R. Song, M. Johnson, S. A. Z. He, C. Milne, X. Wang, I. Lara-Sáez, Q. Xu and W. Wang, *Materials*, 2021, **14**, 5956.
- 28 M. Lei, X. Peng, M. Hu, C. Wan and X. Yu, Research on essential performance of oxidized chitosan-crosslinked acellular porcine aorta modified with bioactive SPP/DOPA for esophageal scaffold with enhanced mechanical strength, biocompatibility and anti-inflammatory, *Int. J. Biol. Macromol.*, 2023, **241**, 124522.
- 29 M. Lavertu, Z. Xia, A. N. Serreqi, M. Berrada, A. Rodrigues, D. Wang, M. D. Buschmann and A. Gupta, A validated  $^1\text{H}$  NMR method for the determination of the degree of deacetylation of chitosan, *J. Pharm. Biomed. Anal.*, 2003, **32**, 1149–1158.
- 30 J. Hoque, B. Bhattacharjee, R. G. Prakash, K. Paramanandham and J. Haldar, *Biomacromolecules*, 2018, **19**, 267–278.
- 31 M. Mahmoudzadeh, A. Fassihi, J. Emami, N. M. Davies and F. Dorkoosh, *J. Drug Target*, 2013, **21**, 693–709.
- 32 A. Salama, *Int. J. Biol. Macromol.*, 2018, **108**, 471–476.
- 33 L. Xing, J. Sun, H. Tan, G. Yuan, J. Li, Y. Jia, D. Xiong, G. Chen, J. Lai, Z. Ling, Y. Chen and X. Niu, *Int. J. Biol. Macromol.*, 2019, **127**, 340–348.
- 34 S. Gou, D. Xie, Y. Ma, Y. Huang, F. Dai, C. Wang and B. Xiao, *ACS Biomater. Sci. Eng.*, 2020, **6**, 1052–1063.
- 35 S. Pan, N. Zhang, X. He, Z. Fang, Y. Wu, Y. Wei and L. Tao, Poly(vinylalcohol) Modified *via* the Hantzsch Reaction for Biosafe Antioxidant Self-Healing Hydrogel, *ACS Macro Lett.*, 2023, **12**, 1037–1044.

